A comparison of thermal infrared to fiber-optic distributed temperature sensing forevaluation of groundwater discharge to surface water

Danielle K. Hare[1,2,*], danielle.hare@aecom.com

Martin A. Briggs[2]

Donald O. Rosenberry[3]

David F. Boutt[1]

John W. Lane[2]

[1]Department of Geosciences, University of Massachusetts Amherst, 611 N. Pleasant St., Amherst, MA, 01003, USA

[2]U.S. Geological Survey, Office of Groundwater, Branch of Geophysics, 11 Sherman Place,Unit 5015, Storrs, CT, 06269 USA

[3]U.S. Geological Survey, National Research Program, Denver, CO USA

*Currently associated with AECOM at Rocky Hill, CT USA.

For resubmission to *Journal of Hydrology* (09/15/2015)

Abstract

Groundwater has a predictable thermal signature that can beused to locate discretezones of discharge to surface water. As climate warms, surface water with strong groundwater influence will provide habitat stability and refuge for thermally stressed-aquatic species, and is therefore critical to locate and protect. Alternatively, these discrete seepage locations may serve as potential point sources of contaminants from polluted aquifers. This study compares two increasingly common heat tracingmethods to locate discrete groundwater discharge: direct-contact measurements made withfiber-optic distributed temperature sensing (FO-DTS) and remote sensing measurements collected with thermal infrared (TIR) cameras. FO-DTS is used to make high spatial resolution (typically m)thermal measurements through time within the water column using temperature-sensitive cables. The spatial-temporal data can be analyzed with statistical measures to reveal zones of groundwater influence, however, the personnelrequirements, time to install, and time to georeferencethe cables can be burdensome, and the control units need constant calibration. In contrast, TIR data collection, either from handheld, airborne, or satellite platforms, can quickly capture point-in-time evaluations of groundwater seepage zones across large scales. However the remotenature of TIR measurementsmeans they can be adversely influenced by a number of environmental and physical factors, and the measurements are limited to the surface "skin" temperature of water features.We present case studies from a range of lentic to lotic aquatic systemstoidentify capabilities and limitations of both technologies and highlight situations in which one or the other might be a better instrument choice for locating groundwater discharge. FO-DTS performs well in all systems across seasons, but data collection was limited spatially by practical considerations of cable installation. TIR is found to consistently locate groundwater seepage

zones above and along the streambank, but submerged seepage zones are only well identified in shallow systems (e.g. <0.5 m depth) with moderate flow. Winter data collection, when groundwater is relatively warm and buoyant, increases the water surface expression of discharge zones in shallow systems.

1. Introduction

Groundwater (GW) discharge to surface water(SW) supportsflow stability and stream habitat, particularly during seasonal low-flowperiods.Upwelling GW often has a thermal, isotopic, and geochemical signature that is distinctly differentfrom thereceiving SW body, and these GW signatures arecomparatively stablethrough time (Hayashi and Rosenberry, 2002). Distinct GWcharacteristics can be used astracers to indicate seepage dynamics; the usefulness of each tracer typically depends on the degree of contrast with SW.Temperatureis a parameter that offers contrast during certain times of the year, as diurnal and annual temperature oscillations strongly influence SW, whereas GW temperatures typically remain near the annual air temperature mean (Constantz, 1998).Therefore, GW seepage zones are oftencooler in summer and warmer in winter than the receiving SW. Yeteven in the transition seasons, when these water end-members are closer in temperature, seepage zones can be identified by reduced thermal variance(Anderson, 2005; Silliman et al., 1995; Stonestrom and Constantz, 2003).In contrast to geochemical tracers, which are often highly variable in space, the GW temperature end-member can be readily identified and/or predicted for a given area (Anderson, 2005; Thoreau, 1854). Temperature measurements are relatively easy to collect and interpret, and recent advances in direct and remotely-sensed temperature measurements have allowed heat tracing to be applied from m to km scales.

Temperature is an indicator of GW seepage as well as acritical SWecological parameter; many aquatic species of commercial and recreational interest survive within a thermal rangethat may be exceeded episodically during summer low flows.In response to a warming climate (Cook et al., 2013; Orr et al., 2015),many temperate streams will continue to warm (Isaak et al., 2011).Stream sections moderated by strong GW influence will likely provide some of the most stable future aquatic habitat(Snyder et al., 2015).In streams with small contributions ofGWdischarge,unmixed thermal anomalies will be more locally important. These localized zones create thermal refugia that are critical to the survival of thermally stressed species,particularly during extreme events (Brunke and Gonser, 1997; Ebersole et al., 2003). Preserving and potentially augmenting areas of thermal refugia is a topic relevant to ongoing and future fisheries management strategies(Kurylyk et al., 2014).Although thermal refugia are most relevant when SW is warmest, fish may also seek out GW upwelling zones when spawning in late-fall to promote egg survival when GW is relatively warm (Geist et al., 2002).

Not all unmixedGW inflows will serve as refugia. GWquality in seepage zones can be impaired if the contributing aquifer is contaminated or has properties that provide unsuitable habitat (Briggs et al., 2012; Conant Jr, 2004; Krause et al., 2013; Weatherill et al., 2014). When an adjacent shallow aquifer is contaminated, areas of focused GW seepage become pollution point-sourcesthat can discharge significant chemical mass-flux into SW. For example, Briggs et al. (2012) used heat tracing methods to locate a contaminated GWseepage zone in Syracuse, NY,and estimated a mass–loading of over 100,000 metric tons of chloride to a stream over a 13 year period.

Researchers use a variety of temperature-sensing technologies to investigate aquatic systems.Direct temperature measurements can be made within the water column or along the streambed, whilethe temperature of the water surface (“skin”) can be evaluated remotely using thermal infrared (TIR) cameras. Because there are inherent spatial scale and data collection efficiency trade-offs between different methods, several thermal methods are often used in concert(Briggs et al., 2013; González-pinzón et al., 2015).Thermal methods commonly used across increasing spatial scales are (1) snapshot-in-time point-scale measurements (Conant Jr, 2004; Ebersole et al., 2003; Lautz and Ribaudo, 2012);(2) point-scale temperature logging through time(Constantz et al., 1994; Daniluk et al., 2013; Hatch et al., 2006; Kelleher et al., 2012; Lautz et al., 2010; Leach and Moore, 2011); (3) longitudinal “Lagrangian” drag-probe surveys (Gendaszek, 2011; Lee, 1985; Vaccaro and Maloy, 2006); (4)fiber-optic distributed temperature sensing (FO-DTS) (Henderson et al., 2009; Selker et al., 2006; Tyler et al., 2009);and (5) TIRdata collected by ground, airborne, and satellite systems (Banks et al., 1996; Baskin, 1998; Deitchman and Loheide, 2009; Handcock et al., 2006; Whiting, 1984). FO-DTS and TIR can be used to collect data over large areas and, therefore, arewell-suited for stream-reach (10’s of m) to basin-scale evaluations of GWdischarge. For example, (Dugdale et al., 2015) used airborne TIR to map potential thermal refugia over approximately 700 km of Canadian streams, the occurrence of which was related to geomorphic variables. However, one primary difference between the two technologies is the location of the measurement: FO-DTS measurements are typically madealong a submerged lakebed or streambed, whereas TIR is a surface measurement sensitive onlyto ground temperature or watersurface skin temperature.

A common use of FO-DTS deploys fiber-optic cables to collect continuous temperature data along the streambed interfaceto identify zones of GW seepage based on temperature anomalies (Briggs et al., 2012; Krause et al., 2012; Selker et al., 2006; Westhoff et al., 2007)and/or thermal variance (Lowry et al., 2007; Selker et al., 2006).Other studies have applied temperature signal analysis methods to assess SW/GW exchange and quantify temporal variability in response to dam operations and tides (Henderson et al., 2009; Mwakanyamale et al., 2012). A commonly used FO-DTS method utilizes the Raman-spectra backscatter of laser light emitted along optical fibers to evaluate temperature (Dakin et al., 1985),withspatial samplingtypically as fine as1.0 m. Linear distance along the sensor cable is determined using the known speed of light transmission and the timing of backscatter arrival. Due to inherent light loss in glass fibers, temperature-dependent anti-Stokes frequency data are scaled to the Stokes frequency data to determine temperature along the fiber. Random noise increases with distance due to attenuation of the light signal along the fiber; therefore, the range of most commerciallyavailable FO-DTS systems is currently limited to approximately 6 km of total fiber length, although greater distances are possible (Selker et al., 2006).FO-DTS data are unique in the fact that data precision is a function of integration distance (measurement increments along the fiber) and time (stacking), and therefore precision is in-part user defined(Tyler et al., 2009);a typical value is approximately 0.1 ˚C. Although FO-DTS measurements are direct, the cable and adjacent streambed sediment can be thermally affected by penetration of solar energy through the water column(Neilson et al., 2010).Mobile bed material can either bury the cable or separate it from the bed, complicating data interpretation (Sebok et al., 2015). FO-DTSalso can require significant effort to install andgeoreference.

TIR data are typically collected within the 8-14 μm“long-wave” radiation range. TIR dataindicate the temperature of an object’s surface scaled by the object’s surface emissivity; emissivity values of natural waters are typically close to 1 (Handcock et al., 2012).Data are obtainedin the form of discrete quantitativeimages or video using handheld (Andrews et al., 2011; Briggs et al., 2013; Cardenas et al., 2008; Schuetz and Weiler, 2011), manned airborne (Dugdale et al., 2015; Loheide and Gorelick, 2006; Rayne and Henderson, 2004; Sheibley et al., 2010; Torgersen et al., 2001),and unmanned airborne systems(UAS) and satellite-basedinstrumentation (Anding and Kauth, 1970; Handcock et al., 2006; Parkinson, 2003).Similar to FO-DTS data, TIR data are used to identify thermal anomalies or gradients in temperature throughout aquatic systems, but data collection with TIR may be much less labor-intensive,and larger-scale surveys are much more practical and efficient.However, using thermal variance to identify inputs of constant temperature (GW) is not commonly done with TIR as spatially consistent temporal data are more difficult to collect, and most surveys are “snapshot” in nature. Further, the “surface-skin” temperature evaluated by TIR may not reveal submerged seepage zones, and are subject to the confounding effects of reflection from surface features (e.g. surface vegetation, bank shadow, sun-glare, etc).

Due to resource and time limitations, environmental research, habitat, and remediation studies often have to choose between an effort-intensive submerged thermal monitoring system (e.g. FO-DTS) and remotely-collected TIR when evaluating the distribution of GW seepage to SW.We hypothesize that the snapshot (in time) and surface-skin nature of most TIR data will limit GW seepage detection in many streams; but under the right set of conditions TIR will detail similar seepage dynamics to submerged FO-DTS, for a fraction of the effort. In other types of SW not as easily covered with fiber optic cables (e.g. peatlands), TIR may more reasonably provide a spatially distributed understanding of seepage processes.We present several case-study examples from a range of lentic and lotic systems and compare seepage evaluations made with the two technologies to better define their respective strengths and optimal applications.

2. Field sites description

Case-study field sites range from a cranberry peatland with 1st-2nd order streams, to small and large rivers, and to two large lakes; all sites have zones of known GW seepage to SW. Regional GW temperature at all sites is expected to range from approximately 9-12 $^{\circ}$C.

2.1 Tidmarsh Farms Cranberry Peatland

Tidmarsh Farms served as a cultivated peatland (2.5 km^2) from the early 1900s until cranberry farming operation ceased in 2010. The kettle hole peatland complex is located in Manomet, Plymouth County, Massachusetts, USA (Figure 1) and is representative of legacy cranberry farming in the area. The site is being actively restored to improve ecological function and enhance human recreational use (Living Observatory at Tidmarsh Farms, Manomet, MA). Tidmarsh Farms drains a small 5 km^2 surficial watershed,yet is a discharge location for the 360 km^2 Plymouth-Carver-Kingston-Duxbury aquifer; therefore, strongGW seepage is anticipated within this site.GW seeps feed numerous surface channels of varied discharge (approximately <1-200 Ls^{-1}) that drain northward into Beaver Dam Brook, eventually discharging into Plymouth Bay (Table 1, Figure 2). Parallel drainage ditches (approximately 1m wide by 0.5 m depth) were cut approximately every 35 meters throughout the site;ditches are generally orientedeast-west or north-south within individual peatland segments (Figure 2). Although the drainage ditches alter the SWhydraulics of the site, these ditchesprovide an opportunity to sample and map surface and GWtemperature in a more regular and well distributedmannerthen would be possible in a natural peatland(e.g. Lowry et al., 2007).

2.2Quashnet River

The lower stretch of the Quashnet River in Waquoit Village, Massachusetts, USA is directly upstreamof U.S. Geological Survey (USGS) stream gage #011058837, below which the river meets the ocean at Waquoit bay (Figure 1).Approximately 2.7 km upstream of the gage, the Quashnet River enters a restricted valley through glacial sand and gravel depositsthat consistently discharge GW to the river.This year-round seepage at approximately 11 $^{\circ}$C creates some of the best brook trout habitat on Cape Cod (Barlow and Hess, 1993) and is therefore the site of trout habitat restoration activities since 1975.Strong GW discharge maintains much of the stable annual flow regime of 493 +/- 147 Ls^{-1} (USGS gage #011058837 monthly data 1988-2012), making this a rather large 1st-order stream (Table 1). The stream was channelizedfor agricultural use (cranberry farming), particularly along the 2 km upstream of the USGS gage; although farming operations ceased in the 1950s the stream remains predominantly channelized and fast flowing with an average bankfull width of approximately 4 m.

2.3 Delaware River

The upper Delaware River is 5th-order, and drains approximately 4700 km^2 of New York and Pennsylvania (Figure 1). River discharge in this region is dam-regulated and generally ranges 28−34 $m^3 s^{-1}$during summer low-flows (USGS gage: 01427510, Callicoon, New York)(Table 1).The area of study is located in the town of Equinunk, PA, USA along a stretch of river that is approximately 100 m wide. Similar to the Quashnet River and Tidmarsh Farms, local GW is approximately 11 $^{\circ}$C, providing refuge in seepage zones for thermally-sensitive aquatic life such as the dwarf wedgemussel (Maloney et al., 2012). Dwarf wedgemussel occurrence has been found to coincide with GW seepage zones consisting of focused bank seeps and more diffuse upwelling through the streambed (Briggs et al., 2013).

2.4 Lake settings (Montana & Michigan)

Upper Red Rock Lake in southwestern Montana is a shallow, 11.8 km^2 lake situated in the Centennial Valley near the headwaters of the Red Rock River (Figure 1). The lake is part of a 100 km^2 wetland complex within the Red Rock Lakes National Wildlife(Sharp et al., 2013). The southern shoreline of the lake receives substantial GW discharge from the adjacent Centennial Mountains that change topography abruptly,creating a large hydraulic gradienttoward the lake (Pierce et al., 2014). GW discharges atexposed seepage zonesalongthe southern shoreline and slightly inland, and at submerged 0.5- to 1.5-m-diameter depressions in the lakebed.

Higgins Lake is located in northern Michigan (Figure 1), has a surface-area of 40 km^2 and average depth of 13 m.Strong GW seepage from a wetland area on the north shore forms a short (approximately 150 m) tributary to the lake.Due to the short residence time within the SW channel of the tributary and thick woodland cover, minimal thermal gradient was observed along the channel, and stream discharge enters the lake at the localGW temperature of approximately 9˚C.

3. Methods

Data were collected with a combination of FO-DTS and TIR instrumentation at the Tidmarsh Farm, Quashnet River, and Delaware River sites;FO-DTS data were not collected at the lake sites but other point-scale temperature measurements were made.

3.1 Fiber-optic distributed temperature sensing

At Tidmarsh Farms FO-DTSdata were collected at integrated 15 minute intervals with Sensor Tran Gemini HT control unit in dual-ended mode.The installed cable was 2.5km long and contained two multimode fibers. TheGemini HT unit allows for 1-meter spatial samplingat approximately 0.1˚C precisionusing 15 min integration timescales. FO-DTS measurements are impacted by the ambient temperature of the reference coil within the control unit. As this ambient coil temperature varies through time there is often a dynamic offset between FO-DTS and "true" temperature (Tyler et al., 2009), which typically varies from approximately +/- 0 to 2˚C. For the Tidmarsh experiments, 50-m temperature-offset calibration coils were maintained with a mixed (with air bubbler) ice and/or ambient bath that were compared through time to an independent HOBO Water Temperature Pro v2 Data Logger with 0.2 ˚C accuracy (Onset Computer Co, Bourne, MA, USA).FO-DTS temperature at every meter along the cable was then corrected for the dynamic offset at every timestep through using the offset pattern observed in the known temperature bath. The known temperature baths were also used to calibrate for signal-loss with fiber distance using the integrated Gemini software; this step is necessary during single-ended FO-DTS data collection, but is automatically accounted for in double-ended data collection. Data for each FO-DTS deployment (n=4) were collected for a minimum of 5 days to ensure multiple diurnal sequences were captured to support thermal variance analysis. Three of the deployments were located on the western portion of the property, one each on the north, central, and southern portions. The remaining deployment was on the eastern portion through the main tributary. Heavy vegetation mats and macrophyte growth at Tidmarsh Farms made it difficult to install and keep the cable in contact with the streambed interface.Regular maintenance of the deployments was required to ensure the cable remained on streambed.

For the Quashnet and Delaware River studies, FO-DTS measurements were typically collected at 4-min intervals and 1.0 m linear sample resolution withan Oryx model SR Remote Logging DTS Unit (Sensornet Ltd.).Calibration for thermal drift was performedin real time using a continuously mixed (and replenished) icebath, which was monitoredusing the integrated T-100 Oryx FO-DTS thermistor. A 30-m+ length of calibration cable was immersedin each icebath, and the standard deviation of FO-DTS temperature within the ice bath over time was used to estimate system precision at 0.1°C for both installations. One-km stainless-steel reinforced cables housing two multimode optical fibers were installed along the streambed using the ambient weight of the cable to maintain contact with the bed.Flat river stones were additionally placed over the cable where necessary.Two cables were installed along the Quashnet River with the control unit in the middle in an effort to cover the most stream length (Figure 3).One cable was installed in a looped pattern at the Delaware River site both directly over and upstream of a known mussel bed

(Figure 4).Both systems were run in double-ended mode, allowing bi-directional data collection that simplifies calibration using the Oryx system software.

In addition to the 1-km cable at the Delaware River, the 4-channel FO-DTS system was simultaneously used to collect data along a vertical axis by wrapping portions of the fiber-optic cable around a 1-m length of PVC pipe to create a high resolution temperature sensor (HRTS) (e.g. Briggs et al., 2012b).An array of five 1-m long HRTS sensors with 0.014 m vertical spatial resolution were emplaced at least 0.4 m into the streambed with the remainder extending vertically into the surface-water column.The array was aligned normal to shore, with 2 m spacing between vertical sensors, starting 2 m from shore at $HRTS_1$ (Figure 5).The intersection of the array plane and the stream bank coincided with a known focused streambank seep of 11°C GW discharging at 129.0 m^3 d^{-1}.Data collected along the HRTS array were of the same temperature resolution and cable-distance integration as the longitudinally deployed cable; for further details please refer to Briggs et al., (2013).

FO-DTS data were collected at Tidmarsh Farm from July –August 2013, at the Quashnet River from July 26-28, 2013, and at the Delaware River July 18-23, 2012. Data for all sites were analyzed in Matlab and visualized with Google Earth Pro (Mountain View, CA).

3.2Thermal Infrared imagery

Hand-held TIR data at Tidmarsh Farms, the Quashnet River, the Delaware River, and Higgins Lakewere collected using a combination of cameras manufactured by FLIR Systems, Inc. (Wilsonville, Oregon) provided by the USGS Office of GW, Branch of Geophysics.TheFLIR T620bx and T640bxmodels collect 640×480 pixel images with a reported 0.04°C sensitivity and calibrated accuracy within 2°C of the true temperature.Both cameras record the image orientation, but the T640bx can also embed internal GPS data into the image metadata.An emissivity of 0.97-0.99 was used for all TIR surveys. Custom programs were developed in Matlab (Mathworks Inc.) to automatically plot T640bx images on a base map according to the position the images were collected.The lower-cost FLIR i7 camera was also used for comparative purposes at the Quashnet River and Tidmarsh Farm sites.The i7 collects 140×140 pixel images with reportedresolution< 0.1 ˚C and calibrated accuracy within 2˚C of the true temperature.Hand-held TIR data were collected at Tidmarsh Farm on November 23, 2012, July 30 and 31 2013, March 21, 2014,and June 11 2015; at the Quashnet River on August 1, 2013 and March 21, 2014; at the Delaware River on July 22, 2012; and at Higgins Lake on June 17, 2014.

Airborne TIR data at Upper Red Rock Lake the lake sites were obtained from an UAS (RQ-11A Raven). Frame-imagery collected at Upper Red Rock Lake was captured from an analog aircraft video stream, geo-referenced, and merged (Todd Preston, written communication). The UAS TIR data are uncalibrated, but show relative differences in temperature using a gray-scale where whiter colors are colder.

3.3 Supporting data collection

At the Quashnet River and lake studies, GW seepage was quantified in discrete locations by using low-profile seepage meters designed for use in flowing water. Installation and field use was completed in accordance with Rosenberry (2008).At all sites except for Upper Red Rock Lake, point temperature data in both the water column and bed were collected using a traceable digital thermometer (Traceable Digital Thermometer (Control Company)) with 0.001˚C resolution, 0.05˚C accuracy. Thermal data associated with the seepage meter location at Upper Red Rock Lake were collected with iButton thermal loggers (Maxim Integrated DS1920). Differential gaging of SWdischarge was performed at Tidmarsh Farms with a Marsh

McBirneyFlo-Mate 2000, and at the Quashnet River with a Flow Tracker (SonTek) Acoustic Doppler Velocimeter.

4. Results

TIR, FO-DTS data, and results of supporting methodsare presented below by site location.

4.1 Tidmarsh Farms Cranberry Peatland

The FO-DTS and TIR surveys completed over the same time period in July 2013identified similar patternsof stronger discrete seepage at focused points located to the peatland interior (Figure 2).At numerous other locations, slower flowing, diffuse seepage was indicated by approximately 11 $^{\circ}$C temperatures, which are warmer than the regional GW flow, indicating longer residence time in the shallow subsurface near the sediment-water interface and, therefore, greater influence of downward heat conduction (Briggs et al., 2014). The presence of the abundant GWseepages observed with these methods was supported by a differential gaging survey along the main stream channel to which the GW drainage ditches discharge that indicated a net GW gain of 130 Ls^{-1}, or approximate 46% increase compared to discharge upstream of the discrete GW discharge areas.Some diffuse submerged seepage zones, particularly in more stagnant drainage ditches, were only visible in summer after the water column was artificially mixed by walking through the area during the TIR survey. Further follow-up TIR surveys in winter conditions showed similar seepage dynamics to summer, but with detection of additional diffuse, low-flux zones, which were likely more visible due to the relative buoyancy of warmer GW (Figure 6).

Both high- (FLIR T640bx, Figure 7a) and low-resolution (FLIR i7, Figure 7b) TIR cameras were able to capture thermal anomalies associated with higher flux seepage dynamics

(Figure 7), although diffuse seepage closer to the SW temperature was more difficult to identify with the i7 model. Further, the i7 data collected in winter often showed an unreasonable range in temperatures that differed from direct measurements, indicating the measurements were less-accurate than the manufacturer-specified 2°C calibrated range (Figure 7b).

4.2 Quashnet River

TIR data collected along the Quashnet River indicated ubiquitous GW seepage through the streambank just above the stream surface, particularly for the downstream section of the stream at the base of steeper topography (Figure 8).These patterns were observed in summer (Figure 8a) and winter (Figure 8b), and inboth seasons the unmixed GW(surface) thermal signature disappeared within cm of a respective bank.FO-DTS data show a general reduction in mean interface temperature and variance at the streambed with downstream distance, due to the net effect of GW discharge bringing in cold water along the entire stream reach (Figure 3a).Thisbias in variance data was detrended so the damping effect offocused streambed seepage could more reasonably be compared with distance (Figure 3b, 3c). The resulting spatially orienteddata show 10s of cold anomalies with relatively low variance along the downstream section, and many-fewer of these points along the upstream section (Figure 3c).

The interpreted pattern of increased GW seepage with distance is supported by net SW gains determined with differential gaging that indicated streamflow increased by 10.0 Ls^{-1} over the upper section, and a further 130.0 Ls^{-1}over the lower section.The very-high net seepage rates observed along the lower reach are enhanced in part by the dozens of relic drainage ditches from previous cranberry farming that drain local GW to the main channelized river section, similar to Tidmarsh Farms. There was seemingly little spatial correlation between the direct streambed seepage patterns observed with the FO-DTS system and the streambank and waterline seepage observed with TIR.Even in winter, there was essentially no water skin expression of focused buoyant streambed seepage determined with FO-DTS, and only a general longitudinal gradient in mixed water column temperature could be observed in addition to the exposed bank seepage using TIR.

4.3 Delaware River

At the Delaware River site, several discrete bank seeps at or near GW temperature were noted using TIR, being at least 10 ˚C colder than other wet bank material. The locations of these seeps coincided with an area known to support one of the few remaining dwarf wedgemussel communities in the upper-Delaware River(Briggs et al., 2013).The largest seep created a thermal anomaly along the bank that was several meters across, but the surface signal dissipated quickly upon entering the river, such that it was undetectable by approximately 2 m from shore (Figure 5a).HRTS data collected with the FO-DTS system along a vertical transect revealed the seep water plunged to the streambed interface, forming a consistent cold-water plume extending approximately 7 m from the bank (Figure 5b).Mean temperature within this plume was approximately 8˚C colder than mixed river water; this pattern was also reflected in the underlying streambed sediments.

The FO-DTS cable was distributed across the streambed parallel to the shoreline.The cable passed through the plume area, then circled back upstream in slightly deeper water forming two approximately parallel transects (Figure 4).Mean temperature along the cable clearly showed the influence of the plunging seepage, which was indicated by a cold, less variable anomaly.In addition, a larger, slightlycolder than SW zone was identified along the central area of the length of cable closer to shore (seen as orange in Figure 4); this zone coincided with the observed expanse of mussels as surveyed in 2012 (written communication Jeffery Cole, USGS, 2013).Overall,variance of the FO-DTS data seemed to be strongly controlled by SW depth except right at the location of the plunging streambank seepage, as there is a decrease in variance in the transect furthest from shore.

4.3 Lake Settings

Gray-scaleinfrared (analog) imagery collected with UAS on August 11, 2011, at Upper Red Rock Lake displays colder GW seepage as whiter areas (Figure 9a).A major seepage feature islocated in an area approximately 10 by 15 m at the shoreline where a spring 7 m inland of the shoreline discharges at approximately 27 m^3d^{-1}. About 30 m from shore in water 0.5 m deep, a 1-m-diameter seepage zone noted by a depression in the lakebed discharged at 3.12 md^{-1}, as evaluated with a seepage meter (Figure 9b). Temperature collected directly at the lakebed in this depression was 8.9 °C, yet it was 18.5 °C on the lake surface. Therefore density-driven thermal stratification kept cold GWat or just above the lake bottom,and prohibited the detection of this strong seepage zone with airborne TIR.

Cold water from the GW-fed tributary created a relatively large anomaly approximately 6m across at the confluence with Higgins Lake (Figure 10), similar to that observed at Upper Red Rock Lake (Figure 9a), although the data resolution with the hand-held camera was much higher (e.g. 307,200 pixels) and temperature measurements quantitative.The unmixed seepage extended approximately 17 m out into the lake, with the surface signature quickly decreasing in size with distance from shore.Fine waveaction caused this plume to be constantly changing in shape and size, but the overall visible length seemed consistent.Direct measurements with a digital thermometer made within the water column and along the bed of the lake indicated that the plume was plunging, extending much farther from shore than was evident from the surface skin (TIR) temperature.

5.Discussion

When deploying TIR or FO-DTS technology many site-specific factors control the "success" of seepage evaluations. The overarching controls including SW characteristics, the spatial distribution of seepage (submerged vs. exposed, diffuse vs. discrete), the seasonality of data collection (relative density of GW to SW), and whether temporal data are collected, often strongly influence survey results. Through this discussion, we explore realized benefits and limitations of TIR and FO-DTS across a range of site conditions with the goal of quantifying thelocation and qualitatively evaluatingflux of GW seepage to SW systems.

5.1 The impacts of seepage spatial distribution and SWcharacteristics

Identifying GW seepage is strongly dependent on the temperaturedifference between SW and GW, and previous work indicates that only relatively strong discrete GW seepage relative to SW discharge (e.g. approximately 2% of SW flow)may be expected to measurably modify mixed SW temperature (Briggs et al., 2012; Lauer et al., 2013).Therefore, the success of FO-DTS and TIR in finding less than 2% additions of low to moderate seepage (e.g. < 1 md^{-1} vertical flux to stream) zones primarily depends on locating the GW thermal signature before complete SW mixing. Under controlled flume conditions,Roshan et al., (2014) found that an empirical relation to quantify GW seepage could be developed based on the apparent temperature response of FO-DTS measurements made along the streambed interface, although this quantification would likely be more difficult in uncontrolled natural settings. We therefore suggest use of TIR and FO-DTS for spatial identification of GW seepage locations, with qualitative comparison of relative seepage rates based on the magnitude and other characteristics of thermal anomalies.

Submerged seepage zones were only well characterized by TIR in the small streams and drainage ditches of the Tidmarsh Farms peatland. We attribute thesimilarity of seepage characterizations made with FO-DTS and TIR methods at Tidmarsh to the shallow depth of water (typically less than 0.5 m), and the low stream discharge (0.002-0.2 m^3s^{-1}) (Table 1). The combination of shallow water and low stream flowreduces thermal stratification induced by density differences between SW and GW (similar to seepage in still lake water, Figure 9), and induces minimal local mechanical mixing and thermal dispersion, thus allowingthe seepage thermal signature to propagate to the water surface for identification with TIR without thermal dilution.Conversely, the deeper, fast flow of the Quashnet River extinguished the thermal influence of focused, submerged GW seepage in close proximity to the streambed interface. A 200 m section of the FO-DTS cable was temporarily suspended at approximately half the total stream column depth in a zone of multiple discrete seepage zones observed along the interface downstream of the control unit (Figure 3).Whenthe cable was suspended in the water column (approximately 0.5x depth),*none*of the previously-observed streambed interface thermal anomalies indicating seepage zones were visible in the FO-DTS data.This result indicates that locating submerged seepage zones along the streambed interface will be a challenging target for TIR in deep, fast flowing water; when using direct-contact methods such as FO-DTS cable, placement will be paramount and caution must be used when assuming the linear measurements made along streambed cables to be representative laterally across the bed(Sebok et al., 2013). Further, the cable suspension experiment indicates that fast flowing water may be a stronger control on reducing water column groundwater thermal influence than depth, so TIR methods may be challenged to locate submerged seepage in the fast, shallow headwaters important to fish habitat.

When GW seepage emerges on exposed banks and at the waterline, TIR may be the most appropriate tool for efficient identification, as FO-DTS cables are not typically installed in such locations.But as in the case of submerged seepage zones, low, shallow flow may make TIR and FO-DTS most comparable in terms of locating GW discharges. Bank seepage at Tidmarsh captured with TIR (e.g. Figures 2b, 6, 7) was also captured by the FO-DTS cable installed along the streambed interface (Figure 2a), as reduced mixing in the shallow channels allowed the GW signal to propagate through the water column to the interface cable. Even in the large Delaware River, shallow (20-40 cm), slow flowing side waters allowed discharge from a strong bank seep (5a) to be captured by a linear FO-DTS cable installed several m from shore (Figure 4).However, extensive exposed bank seepage at the Quashnet River observed with TIR (Figure 8) was not captured by the FO-DTS cable, due to fast and deeper flow. Clearly at the Quashnet River TIR and FO-DTS captured different GW seepage distributions, with TIR efficiently locating exposed bank and waterline seepage, and FO-DTS defining submerged seeps along the streambed.

Although slower flowing, shallow water may enhancea water surface thermal signal for both submerged and exposed bank seepage, relatively still water can obscure seepage signatures, particularly during summer when surface water is warm.Density-driven stratification of relatively cold seepage at Upper Red Rock Lake prevented a thermal signal from reaching thesurface even with a very strong seepage rate (3.12 md^{-1}) and water only 0.5 m deep (Figure 9). This is among the largest seepage rates reported in the literature for lake settings (Rosenberry et al., 2015), so more typical, smaller fluxes likely would not be identified with TIR when lake water is warm. TIR-identified seepage along the margins of Red Rock Lakepresumably plunged toward the lakebed because thermal plumes did not extend more than approximately10 m from the shoreline (Figure 9a), similar to the GW plume observed along the margin of the Delaware River (Figure 5b). GW plunging below the warmer SWwas also a dominant feature of shoreline seepage observed at Lake Higgins (Figure 10). These examples indicate seasonality of data collectionin addition to depth of the water column plays an important role in the sensitivity of various methods to GW seepage, as depending on the time of year, GW may have greater or lesser density than SW. The impact of seasonality on these temperature methods is further explored in section 5.2.

FO-DTS was the superior method for locating exact seepage locations at the channel-scale, while the TIR data often more broadly identified zones of seepage influence at Tidmarsh Farms. For example, FO-DTS and TIR data collected along a 60 m drainage ditch in the summer both clearly identified the channel as a strong seepage zone due to the overall anomalously-cold temperature (Figure 11). However, based solely on the snapshot TIR image, it is difficult to ascertain if seepage occurs along the entire ditch length or whether downstream temperatures are simply influenced by a more spatially discrete upstream seepage source (Figure 11c). In contrast, the analysis of the FO-DTS time series shows stronger variance in daily temperature with downstream distance, indicating a discrete upstream source (Figure 11 a,b). Interestingly, in very shallow SW (0.2m) at Tidmarsh in late winter, focused GW discharge through mm-cm scale macropores (e.g. Menichino et al., 2014) was visible with TIR over a broad area(Figure 12); this type of fine-scale characterization of preferential GW flow is likely not currently possible with any other thermal method. Video of similar fine-scale macropore discharge was also collected in summer along the main channel margin adjacent to a much larger discrete seepage point (Video 1) emphasizing the fine scale seepage processes that would not be captured with higher resolution methods.

5.2 Seasonality of data collection

The smallest temperature differences between SW and GW occur during the transition seasons of spring and autumn. Use of heat to characterize seepage distribution is inherently less sensitive during these times, althoughvariance in thermal time series data can still indicate GW influence (discussed in section 5.4).During the summer and winter seasons of higher heat tracing sensitivity, there is a trade-off in expected thermal characteristics, predominately driven by thermally induced density differences. As shown in Section 5.1, density driven stratification and plunging of GW seepage limits the water surface seepage footprint, particularly in lentic or very slow-flowing water. In these summer situations, TIR will not perform well for submerged seepage, and the seepage footprint of bank seepage entering the water column will be limited. Bank vegetation, floating aquatic vegetation, and leaf cover can obscure airborne TIR, although hand-held data collection is still possible. However, one important positive feature of late summer or early fall is SW flows are typically at their lowest, potentially exposing more bankside seepage zones that would otherwise be submerged at times of higher flow, as was observed at the Delaware River site.

In winter, GW seepage is relatively buoyant, leading to larger water surface anomalies, such as those observed at the Tidmarsh Farms site (Figure 6). It is likely the plunging plume in the Delaware River (Figure 5) and the stratified lakebed seepage (Figure 9) would have a substantially larger surface expression during cold months before or right after ice cover.TIR video collected at approximately the same strong seepage location at Tidmarsh farm nicely captures this seasonal difference. Video 1shows a GW plume plunging beneath the warmer SW during the summer, while Video 2 shows the warmer groundwater seepage buoyant on the surface of the cooler SW in winter. Additionally, leaf and plant cover may be sparse during winter, potentially allowing a less-complicated thermal signal for aerial surveys. Field campaigns should be planned with care however, as snow and ice cover of banks and the water may block the IR signature of GW; several winter TIR campaigns to Tidmarsh Farms were aborted because most diffuse seepage areas were frozen at the surface. One additional major complication of remote data collection in winter is the non-uniqueness of a warm seepage signal in the aquatic environment. In summer, typically the only natural phenomenon in the temperature range encompassing seepage at these sites (approximately 9-14 °C) is GW seepage, making TIR a conclusive identifier.However, in the winter,solar radiation may warm the surface of bank material to this range even when the air temperature is much less than 0°C, making it more difficult to conclusively or automatically extract seepage zone locations. This issue was encountered in winter at the Quashnet River site, the spatially extensive bank and waterline seepage was difficult to discern from direct solar heating of bank materials during daylight hours. It is therefore recommended the TIR data be collected at night or early morning, a suggestion that also applies to summer data collection as reflection of sunlight may also complicate images of water temperature (Figure 5a). One notable exception to this will be freshwater seepage to brackish and marine environments(Hick and Carlton, 1991; Whiting, 1984). The density-effect of dissolved salts will typically make fresh GW relatively buoyant at all times of the year, indicating remote TIR may particularly applicable to locating shallow submarine discharges (e.g. Sheibley et al., 2010) in critical estuary environments.

5.3Survey Efficiency

There are tradeoffs between practical spatial coverage, effort and resources, and desired data when considering TIR and/or FO-DTS. For example, the Tidmarsh Farms Site is a large 250-acre wetland where no previous hydrogeologic investigation had taken place. There was little concept of the spatial distribution of GW seepage at the site, nor obvious indication of specific areas of interest. In fact, results of the TIR survey indicate that surficial zonespreviously assumed to have active GW seepage due to consistent standing water were instead found to simply be localized low elevation zones. Multi-season hand-held TIR surveys were completed in several short evenings/mornings of work and covered a larger area than the FO-DTS deployments, which took several weeks and a team of people to complete.FO-DTS installation efforts were also hampered by thick vegetation in the drainage ditches that made it difficult to submerge the cable at a consistent depth.

FO-DTS may not be able to capture spatial seepage dynamics in wider streams without complicated deployment patterns, as shown with in the Delaware River dataset. This research along with work bySebok et al. (2013)showed that FO-DTS cables often must be directlylocated at seepage discharge zones, or the seepage signal will not be captured. Soft and mobile bed material can quickly cover cables, reducing thermal variance and indicating upward seepage where there may be none. Furthermore, FO-DTS data acquisition is complex; the FO-DTS instrument must be constantly powered and calibrated with at least one known temperature bath,and the cable must be georeferenced and protected during the deployment.At Tidmarsh Farms, where FO-DTS and TIR data were collected concurrently, a similar distribution of seepage patterns and magnitudes was determined, in accordance with the overarching hypothesis of this work. Therefore, at this low-energy wetland site, where the primary goal of site characterization was to locate and qualitatively compare GW seeps, the fast “remote” TIR survey method was more efficient than the more time- and labor-intensive FO-DTS method.However, at the other aquatic settings presented here, TIR poorly delineated submerged seepage patterns or missed them all together due to the reasons discussed above. If the GW seepage processes of interest are expected to be exposed along banks and the waterline, or in very shallow, low flow environments, TIR will often be the most applicable and efficient technology to utilize.

When comparing TIR and FO-DTS methods it is important to consider the time and resources required to process and interpret the data. FO-DTS produces copious amounts of data, where distance is recorded from the optical signal as length from the unit, which needs to be thoroughly georeferenced to actual field location. This inherently requiresa post-processing phase that can take a significant amount of time before data can be fully analyzed. Conversely, depending on how they are collected, TIR images can be reviewed in real-time and the survey adjusted accordingly. One of the most powerful uses of hand-held TIR data collection is to use the continuous camera display in a "reconnaissance" mode when exploring spatially extensive sites, and then collecting specific data frames and video at points of interest observed in the data feed.

Some TIR instruments such as the FLIR T640bx used here record GPS location of the camera and shot direction in metadata associated with each image, which can be automatically accessed for spatial plotting using programs such as Matlab.Human interpretation is still an important step, as TIR images often are complicated by vegetation cover and reflection. Another consideration is the location of the camera/photographer at the time of the shot will be the recorded GPS coordinates within the metadata on the image, which is likely not entirely coincident with the feature of interest. Additionally, as TIR data are collected as an image, the numerous images that will be acquired after a survey can be cumbersome to view spatially for a whole site. For the generation of Figure 2b, a Matlab based program was developed so that a pixel could be chosen from each figure that represents the thermal interest of that site. This allows for better large-scale visualization and interpretation of this data; making IR results spatially comparable to FO-DTS results (Figure 2). Airborne surveys provide both the challenge and opportunity of collecting large data sets that have similar challenges to manage and georeference as FO-DTS.

Data spatial resolution and precision is also an important consideration when choosing between FO-DTS and TIR technologies. TIR resolution has a large range of resolution available; first, obviously, between satellite/aerial TIR and handheld TIR the spatial scale of each pixel can range from several meters to sub-mm.Presently, payload weight is a limiting factor on the complexity of TIR camerasthat can be flown using UAS-type aircraft (e.g. grayscale images extracted from analog video in Figure 9a), although that technology is improving quickly. For example the small new FLIR Tau2 640 camera can record calibrated digital data, and the instrument weight can be accommodated by some hand-launched UAS aircraft. It is likely that within a few years, adjustments to rules that currently restrict scientific use of UAS TIR by Federal agencies, combined with improved instrumentation and aircraft, will lead to greatly increased use of TIR in truly remote sensing of GW seepage and thermal refugia processes.

Within the handheld class of TIR cameras, image resolution and camera features are reflected in the price, which can range over an order of magnitude between the two instruments showcased in Figure 7. It is shown that both cameras capture similar gross seepage zone locations, although finer mixing patterns between emergent GW and SW is clearly better captured by the more expensive instrument (Figure 7a). A strength of TIR data is that it can be an extremely effective medium to convey complicated GW seepage patterns to cooperators and the public, in which case data resolution also plays a role.FO-DTS data are typically collected at the m-scale, although modified wrapped versions can improve this to the cm-scale over short lengths (Figure 5b). The m-scale is generally adequate to resolve streambed seepage patterns, while the wrapped versions are more applicable to the study of water column mixing and streambed processes.

5.4 Temporal Data

TIR surveys are typically collected as a series of instantaneous images of water “skin” temperature. Although time-lapse functionality is possible using a mounted camera(e.g. Tonolla et al., 2010), longer-term deployment (days+) is difficult, and interpretation is complicated by changes in water surface roughness (wind) and solar reflection. Shorter-term TIR videos can be useful in investigating the mixing of SW and GW at discrete points of seepage, including the stability of thermal refugia. As noted in Section 5.2 video collected at approximately the same location in winter and summer at Tidmarsh Farms is used to directly observe density-driven differences in mixing between surface and groundwater (Video 1, Video 2). Therefore, TIR video offers the potential to both uniquely capture groundwater seepage processes, and communicate these processes to the public and policy makers as a teaching tool.

FO-DTS is designed to collect time-series data, which is one of the greatest strengths of the technology.Even in the transition seasons of spring and fall when SW and GW temperatures are similar, seepage locations typically display lower daily variance in streambed interface temperature due to the consistent temperature GW influence (e.g. Selker et al., 2006) as shown in Figures 3 and 4. Further, subtle hyporheic return flows which often have similar mean temperature to SW,may also be identified in this manner.Variance analysis is useful in revealing diffuse seepage zones which may have less contrast with SW temperature due to greater downward conductive influence (warming) from the surface on upwelling GW (Figure 2a). Without variance analysis, it can be difficult to confirm temperature anomaliesat diffuse, low flux seeps, or artifacts caused by changes in the surface water characteristics.If specific submerged seepage zones need to be pinpointed, time-domain data are also useful (Figure 11b).

Beyond delineatingseepage spatial distribution, one major goal of seepage zone evaluation may be the quantification of seepage magnitude. This has been attempted in specific situations with TIR data (e.g. Pandey et al., 2013), although this approach is prone to error as only surface temperature is evaluated which usually does not reflect “mixed” water column temperature (Handcock et al., 2006). Submerged FO-DTS data are better suited for application to a mixing model, and temporal data can be averaged to improve temperature precision, which is critical, as typically the change in mixed stream temperature due to seepage influence is relatively small. For example, Briggs et al. (2012) used the 2-hr average temperature along a large stream to quantify contaminated GW seepage based on only a 0.3 ˚C change in mixed temperature downstream of a strong seepage zone. Modified wrapped FO-DTS, referred to as HRTS, can be installed vertically in the streambed to estimate fluid flux based on the vertical propagation of diurnal signals (Figure 5b)(Briggs et al., 2013; Briggs et al., 2012). Additionally, investigating water column mixing and the persistence of thermal refugia requires time domain data, particularly when cold GW inputs plunge and stratify in summer (Figure 5). However, as noted previously, TIR surveys can provide for efficient, powerful thermal reconnaissance of a site for installation of in-situ thermaltime-series point measurements or seepage meters.

6. Summary

TIR and FO-DTS data show similar patterns of strong GW seepage in the smaller, shallow, flowing streams of Tidmarsh Farms, but in the larger stream systems data from these methods contrasted greatly. The thermal signature of submerged seepage zones was not present at the water surface in the deeper, faster flowing Quashnet and Delaware Rivers, and therefore not observed with TIR. For similar reasons bank seeps were not identified with FO-DTS, emphasizing the usefulness of these methods combined. At the lake sites where FO-DTS was not collected, known locations of seepage were identified with TIR only when the seepage originated on-shore or at the water-line. However, under typical FO-DTS installations along the thalweg streambed interface bank seepage may not be readily observed, depending on the size and velocity of the stream. These examples make clear that detailed habitat studies may need to consider both remote and direct temperature measurement, in addition to other in-situ methods to fully capture the seepage regime at a site.

Direct-contact FO-DTS and remotely sensed TIR data provide thermal evaluations of aquatic environments, however these fundamentally different types of measurements have varied sensitivity to seepage processes, primarily due to the opacity of water to infrared radiation. Handheld and aerial TIR provides efficient reconnaissance due to the potential simplicity of performing remote surveys over large areas, particularly with the broadening future of UAS data collection. HoweverFO-DTS allows for a more rigorous assessment of the potential seepage rates and distribution of seepage. Overall, FO-DTS provides a more spatially-discrete characterization of GW seepage, often capturing more subtle streambed seepage dynamics including temporal features indicative of seepage zones (e.g. low temperature variance). The exception to this seemed to be very small scale (mm to cm) preferential groundwater discharge in shallow water, which could be mapped with TIR in winter but would be lost in 1-m scale FO-DTS integrated measurements.

When evaluatingthese methods there will inherently be tradeoffs between higher-cost direct measurements made with FO-DTS and potential larger-scale indirect measurements made with TIR. Each site's attributes and study goals must be evaluated uniquely to best decide which method(s)will collect the appropriate data to evaluate GW seepage to SW. In either case thermal sensing at large scales in aquatic systems offers one of the few methodologies to comprehensively locate the discrete GW discharge points that may strongly control SW quality, temperature, and stability in a changing climate.

Acknowledgments

For the Tidmarsh Farms study much thanks is given to Glorianna Davenport and Evan Shulman, Alex Hackman of Massachusetts DER, Christine Hatch, Henry Eshbaugh and Eric Van Dam for data collection, site co-ordination, and their guidance. For the Delaware River study we thank Emily Voytek for help with data collection and interpretation, and Heather Galbraith, Jeffery Cole, Carrie Blakeslee, Celicia Boyden, Chris Peterson, Amanda Lanning, Eric White, Don Hamilton, and Sean Buckley for assistance in the field.For the Quashnet River investigation we thank Jud Harvey, Robert Bradley,Geoffrey Delin, Paul Barlow, Denis LaBlanc, Brendan Buskirk, Celicia Boyden, Sean Buckley, Alex Walker, Yuri Rupert for contributions to field data collection.Hayes Buxton and Rick Sojdaare thanked for field assistance at Upper Red Rock Lake.

Funding for thesestudies was provided by the Tidmarsh Farms Living Observatory, U.S. Geological Survey GW Resources and Toxic Substance Hydrology Programs, and the National Science Foundation (EAR-0901480).Any use of trade, firm, or product names is for descriptive purposes only and does not imply endorsement by the U.S. Government.

References

Anderson, M.P., 2005. Heat as a ground water tracer. Ground Water 43, 951–68.

Anding, D., Kauth, R., 1970. Estimation of sea surface temperature from space. Remote Sens. Environ. 217–220.

Andrews, B.J., Cardenas, M.B., Bennett, P.C., 2011. Analysis of turbulent nonisothermal mixing between a jet and cooler ambient water using thermal imagery. Geochemistry, Geophys. Geosystems 12.

Banks, W.S.L., Paylor, R.J., Hughes, W.B., 1996. Using thermal-infrared imagery to delineate ground-water discharge. Ground Water 34, 434–443.

Barlow, P.M., Hess, K.M., 1993. Simulated hydrologic responses of the Quashnet River stream-aquifer system to proposed ground-water withdrawals, Cape Cod, Massachusetts. U.S. Geol. Surv. Rep. 93-4064 51.

Baskin, R.L., 1998. Locating shoreline submarine springs in two Utah lakes using thermal imagery, in: Pitman, J.K., Carroll, A.R. (Eds.), Modern & Ancient Lake Systems; New Problems and Perspectives. Utah Geological Association, Salt Lake City, Utah, pp. 51–57.

Briggs, M.A., Lautz, L.K., Buckley, S.F., Lane, J.W., 2014. Practical limitations on the use of diurnal temperature signals to quantify groundwater upwelling. J. Hydrol. 519, 1739–1751.

Briggs, M.A., Lautz, L.K., McKenzie, J.M., 2012. A comparison of fibre-optic distributed temperature sensing to traditional methods of evaluating groundwater inflow to streams. Hydrol. Process. 26, 1277–1290.

Briggs, M.A., Lautz, L.K., McKenzie, J.M., Gordon, R.P., Hare, D.K., 2012. Using high-resolution distributed temperature sensing to quantify spatial and temporal variability in vertical hyporheic flux. Water Resour. Res. 48, 1–16.

Briggs, M.A., Voytek, E.B., Day-Lewis, F.D., Rosenberry, D.O., Lane, J.W., 2013. Understanding water column and streambed thermal refugia for endangered mussels in the Delaware River. Environ. Sci. Technol. 47, 11423–31.

Brunke, M., Gonser, T., 1997. The ecological significance of exchange processes between rivers and groundwater. Freshw. Biol. 37, 1–33.

Cardenas, M.B., Harvey, J.W., Packman, A.I., Scott, D.T., 2008. Ground-based thermography of fluvial systems at low and high discharge reveals potential complex thermal heterogeneity driven by flow variation and bioroughness. Hydrol. Process. 986, 980–986.

Conant Jr, B., 2004. Delineating and quantifying ground water discharge zones using streambed temperatures. Ground Water 42, 243–257.

Constantz, J., 1998. Interaction between stream temperature, streamflow, and groundwater exchanges in Alpine streams. Water Resour. Res. 34, 1609–1615.

Constantz, J., Park, M., Thomas, C.L., Zellweger, G., 1994. Influence of diurnal variations in stream temperature on streamflow loss and groundwater recharge 30, 3253–3264.

Cook, J., Nuccitelli, D., Green, S. a, Richardson, M., Winkler, B., Painting, R., Way, R., Jacobs, P., Skuce, A., 2013. Quantifying the consensus on anthropogenic global warming in the scientific literature. Environ. Res. Lett. 8, 024024.

Dakin, J.P., Pratt, D.J., Bibby, G.W., Ross, J.N., 1985. Distributed optical fibre raman temperature sensor using a semiconductor light source and detector. Electron. Lett. 21, 569–570.

Daniluk, T.L., Lautz, L.K., Gordon, R.P., Endreny, T.A., 2013. Surface water-groundwater interaction at restored streams and associated reference reaches. Hydrol. Process. 27, 3730–3746.

Deitchman, R.S., Loheide, S.P., 2009. Ground-based thermal imaging of groundwater flow processes at the seepage face. Geophys. Res. Lett. 36, 1–6.

Dugdale, S.J., Bergeron, N.E., St-Hilaire, A., 2015. Spatial distribution of thermal refuges analysed in relation to riverscape hydromorphology using airborne thermal infrared imagery. Remote Sens. Environ. 160, 43–55.

Ebersole, J.L., Liss, W.J., Frissell, C.A., 2003. Thermal heterogeneity, stream channel morphology, and salmonid abundance in northeastern Oregon streams. Can. J. Fish. Aquat. Sci. 60, 1266–1280.

Ebersole, J.L., Liss, W.J., Frissell, C.A., 2003. Cold water patches in warm streams: physicochemical characteristics and the influence of shading.Journal of the American Water Resources Association,59860, 355–368.

Geist, D.R., Hanrahan, T.P., Arntzen, E. V, Mcmichael, G.A., Murray, C.J., Chien, Y., 2002. Physicochemical characteristics of the hyporheic zone affect redd site selection by chum salmon and fall chinook salmon in the Columbia River. North Am. J. Fish. Manag. 22, 1077–1085.

Gendaszek, A., 2011. Thermal profiles for selected river reaches in the Stillaguamish River Basin , Washington , August 2011. USGS Data Ser. 654.

González-pinzón, R., Ward, A.S., Hatch, C.E., Wlostowski, A.N., Singha, K., Gooseff, M.N., Haggerty, R., Harvey, J.W., Cirpka, O.A., Brock, J.T., 2015. A field comparison of multiple techniques to quantify groundwater – surface-water interactions. Freshw. Sci. 34.

Handcock, R.N., Gillespie, a. R., Cherkauer, K. a., Kay, J.E., Burges, S.J., Kampf, S.K., 2006. Accuracy and uncertainty of thermal-infrared remote sensing of stream temperatures at multiple spatial scales. Remote Sens. Environ. 100, 427–440.

Handcock, R.N., Torgersen, C.E., Cherkauer, K.A., Gillespie, A.R., Tockner, K., Faux, R.N., Tan, J., 2012. Thermal infrared remote sensing of water temperature in riverine landscapes, Fluvial Remote Sensing for Science and Management. John Wiley & Sons Inc., pp. 85–113.

Hatch, C.E., Fisher, A.T., Revenaugh, J.S., Constantz, J., Ruehl, C., 2006. Quantifying surface water–groundwater interactions using time series analysis of streambed thermal records: Method development. Water Resour. Res. 42, 1–14.

Hayashi, M., Rosenberry, D.O., 2002. Effects of ground water exchange on the hydrology and ecology of surface water. Ground Water 40, 309–316.

Henderson, R.D., Day-Lewis, F.D., Harvey, C.F., 2009. Investigation of aquifer-estuary interaction using wavelet analysis of fiber-optic temperature data. Geophys. Res. Lett. 36, 1–6.

Hick, P.T., Carlton, M.D., 1991. Practical applications of airborne multispectral scanner data for forest, agriculture, and environmental monitoring, in: 24th International Symposium on Remote Sensing of Environment. Rio de Janeiro, Brazil, pp. 60–61.

Isaak, D.J., Wollrab, S., Horan, D., Chandler, G., 2011. Climate change effects on stream and river temperatures across the northwest U.S. from 1980–2009 and implications for salmonid fishes. Clim. Change 113, 499–524.

Kelleher, C., Wagener, T., Gooseff, M., McGlynn, B., McGuire, K., Marshall, L., 2012. Investigating controls on the thermal sensitivity of Pennsylvania streams. Hydrol. Process. 26, 771–785.

Krause, S., Blume, T., Cassidy, N.J., 2012. Investigating patterns and controls of groundwater up-welling in a lowland river by combining Fibre-optic Distributed Temperature Sensing with observations of vertical hydraulic gradients. Hydrol. Earth Syst. Sci. 16, 1775–1792.

Krause, S., Tecklenburg, C., Munz, M., Naden, E., 2013. Streambed nitrogen cycling beyond the hyporheic zone: Flow controls on horizontal patterns and depth distribution of nitrate and dissolved oxygen in the upwelling groundwater of a lowland river. J. Geophys. Res. Biogeosciences 118, 54–67.

Kurylyk, B.L., MacQuarrie, K.T.B., Linnansaari, T., Cunjak, R. a., Curry, R.A., 2014. Preserving, augmenting, and creating cold-water thermal refugia in rivers: concepts derived from research on the Miramichi River, New Brunswick (Canada). Ecohydrology.

Lauer, F., Frede, H.-G., Breuer, L., 2013. Uncertainty assessment of quantifying spatially concentrated groundwater discharge to small streams by distributed temperature sensing. Water Resour. Res. 49, 400–407.

Lautz, L.K., Kranes, N.T., Siegel, D.I., 2010. Heat tracing of heterogeneous hyporheic exchange adjacent to in-stream geomorphic features. Hydrol. Process. 24, 3074–3086.

Lautz, L.K., Ribaudo, R.E., 2012. Scaling up point-in-space heat tracing of seepage flux using bed temperatures as a quantitative proxy. Hydrogeol. J. 20, 1223–1238.

Leach, J. A., Moore, R.D., 2011. Stream temperature dynamics in two hydrogeomorphically distinct reaches. Hydrol. Process. 25, 679–690.

Lee, D.R., 1985. Method for locating sediment anomalies in lakebeds that can be caused by groundwater flow. J. Hydrol. 79, 187–193.

Loheide, S.P., Gorelick, S.M., 2006. Quantifying stream-aquifer interactions through the analysis of remotely sensed thermographic profiles and in situ temperature histories. Environ. Sci. Technol. 40, 3336–3341.

Lowry, C.S., Walker, J.F., Hunt, R.J., Anderson, M.P., 2007. Identifying spatial variability of groundwater discharge in a wetland stream using a distributed temperature sensor. Water Resour. Res. 43, 1–9.

Maloney, K.O., Lellis, W. a., Bennett, R.M., Waddle, T.J., 2012. Habitat persistence for sedentary organisms in managed rivers: the case for the federally endangered dwarf wedgemussel (*Alasmidonta heterodon*) in the Delaware River. Freshw. Biol. 57, 1315–1327.

Menichino, G.T., Ward, A.S., Hester, E.T., 2014. Macropores as preferential flow paths in meander bends. Hydrol. Process. 28, 482–495.

Mwakanyamale, K., Slater, L., Day-Lewis, F., Elwaseif, M., Johnson, C., 2012. Spatially variable stage-driven groundwater-surface water interaction inferred from time-frequency analysis of distributed temperature sensing data. Geophys. Res. Lett. 39, 1–6.

Neilson, B.T., Hatch, C.E., Ban, H., Tyler, S.W., 2010. Solar radiative heating of fiber-optic cables used to monitor temperatures in water. Water Resour. Res. 46, 1–17.

Orr, H.G., Simpson, G.L., des Clers, S., Watts, G., Hughes, M., Hannaford, J., Dunbar, M.J., Laizé, C.L.R., Wilby, R.L., Battarbee, R.W., Evans, R., 2015. Detecting changing river temperatures in England and Wales. Hydrol. Process. 29, 752–766.

Pandey, P., Gleeson, T., Baraer, M., 2013. Toward quantifying discrete groundwater discharge from frozen seepage faces using thermal infrared images. Geophys. Res. Lett. 40, 123–127.

Parkinson, C.L., 2003. Aqua: an earth-observing satellite mission to examine water and other climate variables. IEEE Trans. Geosci. Remote Sens. 41, 173–183.

Pierce, K.L., Chesley-Preston, T.L., Sojda, R.L., 2014. Surficial geologic map of the Red Rock Lakes area, southwest Montana. U.S. Geol. Surv. Open-File Rep. 2014-1157, 22.

Rayne, S., Henderson, G., 2004. Airborn thermal infrared remote sensing of stream and riparian temperatures in the Nicola River Watershed, British Columbia, Canada. J. Environ. Hydrol. 12, 1–11.

Rosenberry, D.O., 2008. A seepage meter designed for use in flowing water. J. Hydrol. 359, 118–130.

Rosenberry, D.O., Lewandowski, J., Meinikmann, K., Nützmann, G., 2015. Groundwater - the disregarded component in lake water and nutrient budgets. Part 1: effects of groundwater on hydrology. Hydrol. Process. 29, 2895–2921.

Roshan, H., Young, M., Andersen, M.S., Acworth, R.I., 2014. Limitations of fibre optic distributed temperature sensing for quantifying surface water groundwater interactions. Hydrol. Earth Syst. Sci. Discuss. 11, 8167–8190.

Schuetz, T., Weiler, M., 2011. Quantification of localized groundwater inflow into streams using ground-based infrared thermography. Geophys. Res. Lett. 38, 1–5.

Sebok, E., Duque, C., Engesgaard, P., Boegh, E., 2015. Application of Distributed Temperature Sensing for coupled mapping of sedimentation processes and spatio-temporal variability of groundwater discharge in soft-bedded streams. Hydrol. Process., 29, 3408–3422.

Sebok, E., Duque, C., Kazmierczak, J., Engesgaard, P., Nilsson, B., Karan, S., Frandsen, M., 2013. High-resolution distributed temperature sensing to detect seasonal groundwater discharge into Lake Væng. Water Resour. Res. 49, 5355–5368.

Selker, J., van de Giesen, N.C., Westhoff, M., Luxemburg, W., Parlange, M.B., 2006. Fiber optics opens window on stream dynamics. Geophys. Res. Lett. 33.

Selker, J.S., Thévenaz, L., Huwald, H., Mallet, A., Luxemburg, W., van de Giesen, N., Stejskal, M., Zeman, J., Westhoff, M., Parlange, M.B., 2006. Distributed fiber-optic temperature sensing for hydrologic systems. Water Resour. Res. 42, 1–8.

Sharp, J.L., Sojda, R.S., Greenwood, M., Rosenberry, D.O., Warren, J.M., 2013. Statistical classification of vegetation and water depths in montane wetlands. Ecohydrology 6, 173–181.

Sheibley, R.W., Josberger, E.G., Chickadel, C., 2010. Locating inputs of freshwater to Lynch Cove , Hood Canal , Washington , using aerial infrared photography. USGS Fact Sheet Fact Sheet 2010–3072.

Silliman, S.E., Ramirez, J., Mccabe, R.L., 1995. Quantifying downflow through creek sediments using temperature time-series - one-dimensional solution incorporating measured surface-temperature. J. Hydrol. 167, 99–119.

Snyder, C.D., Hitt, N.P., Young, J.A., 2015. Accounting for groundwater in stream fish thermal habitat responses to climate change. Ecol. Appl. 25, 281–304.

Stonestrom, D.A., Constantz, J., 2003. Heat as a tool for studying the movement of ground water near streams. U. S. Geological Survey Circular 1260.

Thoreau, H.D., 1854. Walden; or, Life in the Woods. Boston: Ticknor & Fields. Ticknor & Fields., Boston.

Tonolla, D., Acuña, V., Uehlinger, U., Frank, T., Tockner, K., 2010. Thermal heterogeneity in river floodplains. Ecosystems 13, 727–740.

Torgersen, C.E., Faux, R.N., McIntosh, B.A., Poage, N.J., Norton, D.J., 2001. Airborne thermal remote sensing for water temperature assessment in rivers and streams. Remote Sens. Environ. 76, 386–398.

Tyler, S.W., Selker, J.S., Hausner, M.B., Hatch, C.E., Torgersen, T., Thodal, C.E., Schladow, S.G., 2009. Environmental temperature sensing using Raman spectra DTS fiber-optic methods. Water Resour. Res. 45, 1–11.

Vaccaro, J.J., Maloy, K.J., 2006. A thermal profile method to identify potential ground-water discharge areas and preferred salmonid habitats for long river reaches Scientific Investigations Report 2006 – 5136. USGS Investig. Rep. Rep. 2006 – 5136.

Weatherill, J., Krause, S., Voyce, K., Drijfhout, F., Levy, A., Cassidy, N., 2014. Nested monitoring approaches to delineate groundwater trichloroethene discharge to a UK lowland stream at multiple spatial scales. J. Contam. Hydrol. 158C, 38–54.

Westhoff, M.C., Savenije, H.H.G., Luxemburg, W.M.J., Stelling, G.S., van de Giesen, N.C., Selker, J.S., Pfister, L., Uhlenbrook, S., 2007. A distributed stream temperature model using high resolution temperature observations. Hydrol. Earth Syst. Sci. 11, 1469–1480.

Whiting, J.M., 1984. The effect of groundwater inflow on evaporation from a saline lake. J. Clim. Appl. Meteorol. 23, 214–221.

Table

Table 1. General surface water characteristics and the type of thermal data collected at each site

site	surface water Q ($m^3 s^{-1}$)	range width (m)	range thalweg depth (m)	TIR data collection platform	FO-DTS data collected?
Tidmarsh Farms, MA	***0.002:0.2***	***0.2:6***	***0.05:0.75***	***handheld***	***Y***
Quashnet River, MA	***0.4:0.6***	***3:6***	***0.2-0.75***	***handheld***	***Y***
Delaware River, PA	***28:34***	***70:110***	***0.3:2.0***	***handheld***	***Y***
Red Rock Lake, MO	***N/A***	***N/A***	***N/A***	***remote airborne***	***N***
Higgins Lake, MI	***N/A***	***N/A***	***N/A***	***handheld***	***N***

Figures

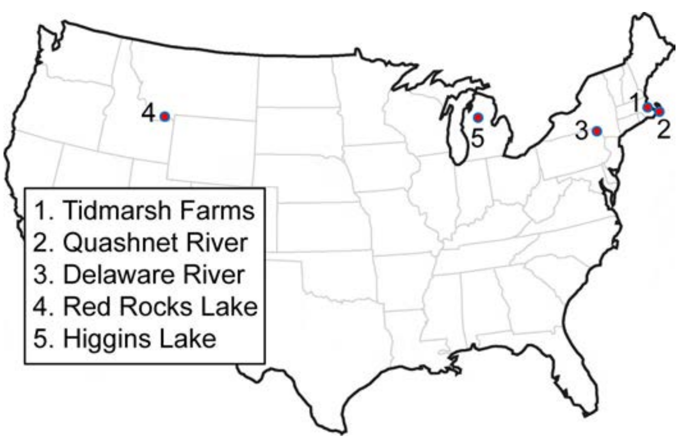

Figure 1.A map of the United States of America showing the general location of each site.

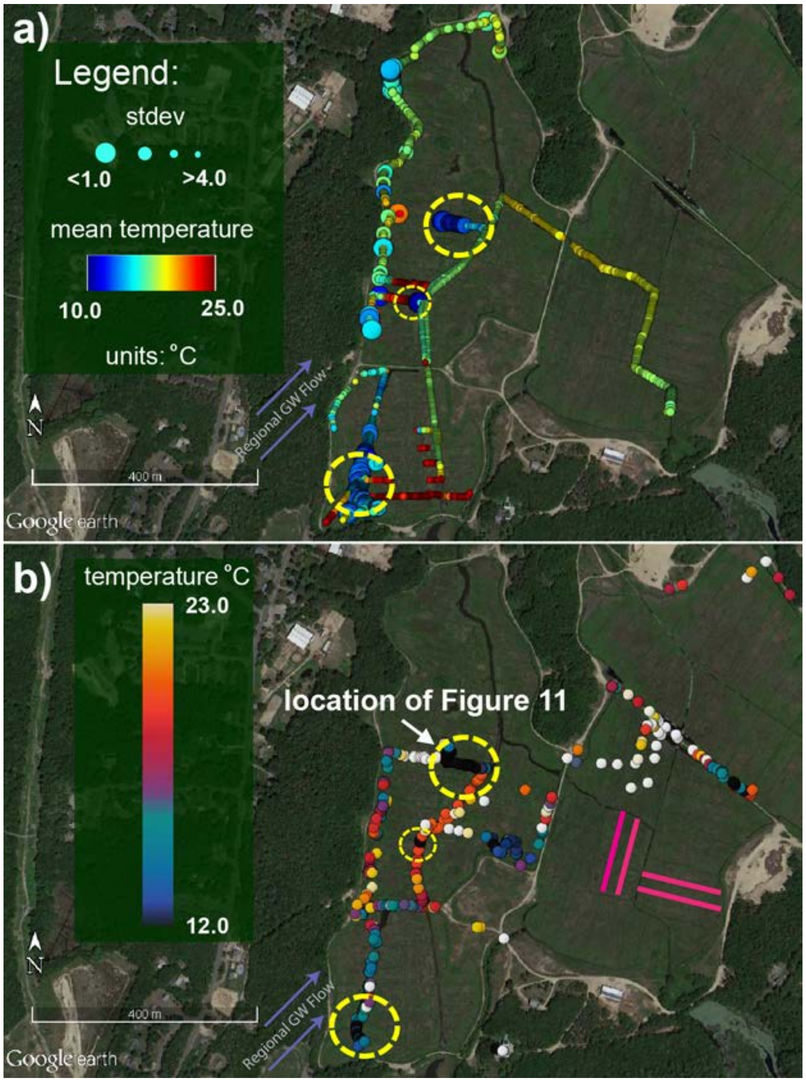

Figure 2.A map of summer 2013 Tidmarsh Farm cranberry bog a)FO-DTS data, and b) TIR data. FO-DTS data are collected through time, so variance analysis can be used to indicate seepage zones (low variance) in addition tomean temperature. The pink lines in the lower-right of panel b) highlight the predominant drainage ditch orrientations at the site and typical spacing. High-flux GW seepage zones were identified similiarly between the two methods (yellow dashed circles), and more diffuse seepage zones were indicated by modified GW temperatures and showed greater variability between the methods.Basemap from Google earth Pro software.

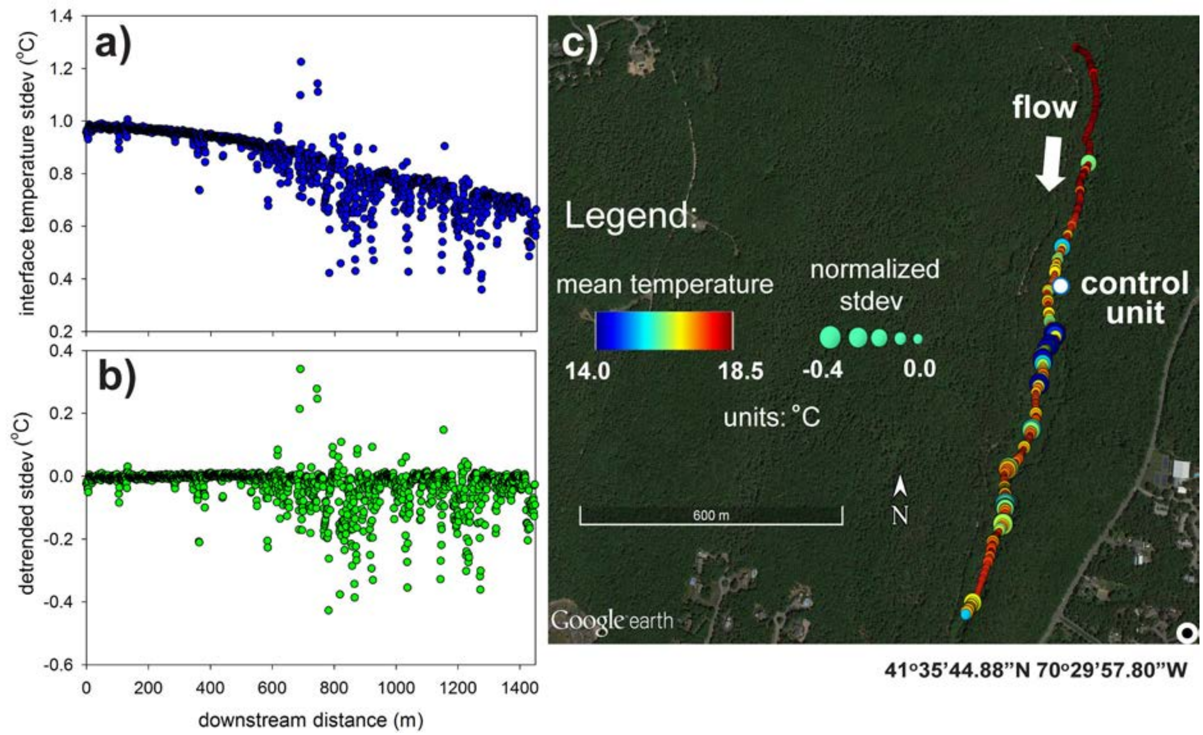

Figure 3.Quashnet River streambed interface temperature over two days in July 2013 as evaluated with FO-DTS shows a) a general trend in decreasing variance with downstream distance with many discrete anomalies of mostly reduced variance; b) the downstream trend in overall reduced variance is removed so anomalies can be more readily compared to indicated relative seepage dynamics; c) The mean temperature along the streambed interface with dot size indicative of detrendedthermal variance.Basemap from Google earth Pro software.

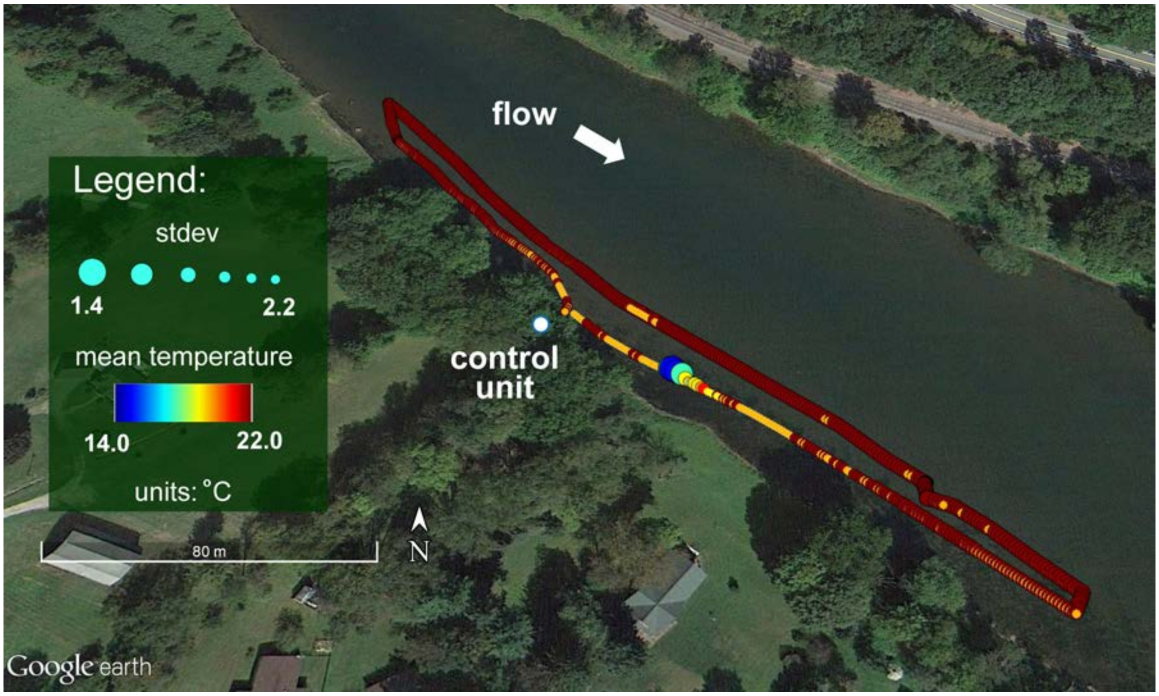

Figure 4. Delaware River streambed interface temperature over two days in July 2012 as evaluated with FO-DTS; as in Figure 2a and 3c the size of each data point is inversely related to thermal variance.Basemap from Google earth Pro software.

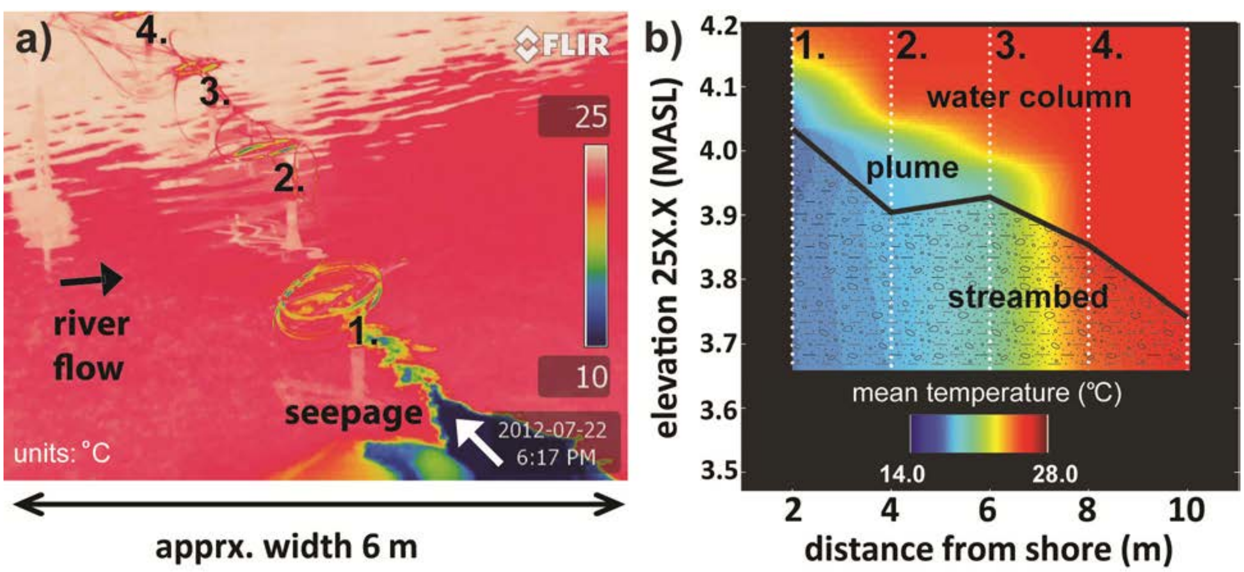

Figure 5. Panel a) shows a TIR image taken at the Delaware River site looking out toward the river from the discrete bank seep, reflected TIR (not river temperature) appears as whiter colors; vertical FO-HRTS profiles were collected at 2 m spacing in a transect normal to shore.The vertical FO-HRTS data were used to b) visualize mean temperature over 5 days across an interpolated 2-D cross-section through the water column into the streambed showing a relatively stable cold plume of plunging GW. These images are modified from Briggs et al. (2013).

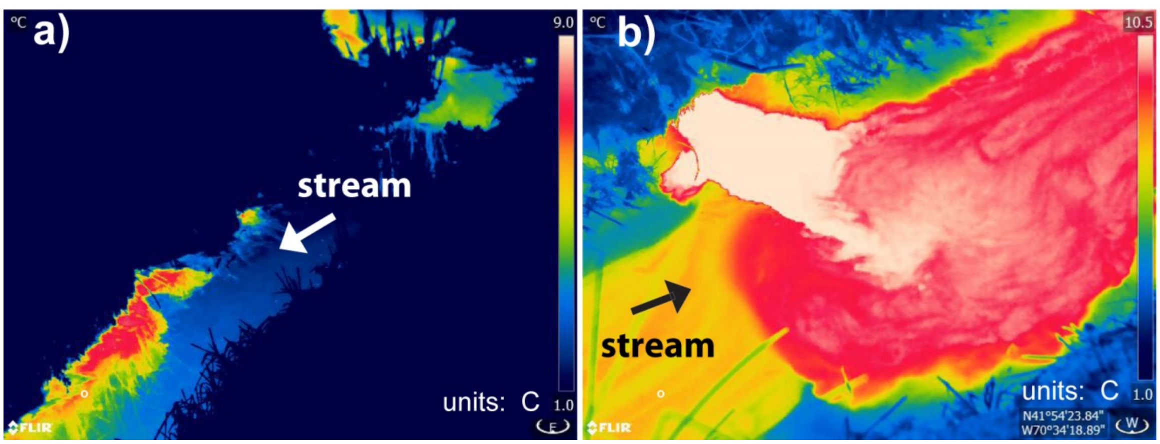

Figure 6.Two TIR images taken from unique locations during the winter at the Tidmarsh Farms Cranberry Farm. These show seepage of relatively warm, buoyant GW entering SW drainage ditches from a) far (image approximately 10 m across at bottom) and b) near (image approximately 0.4 m across at bottom) viewpoints.

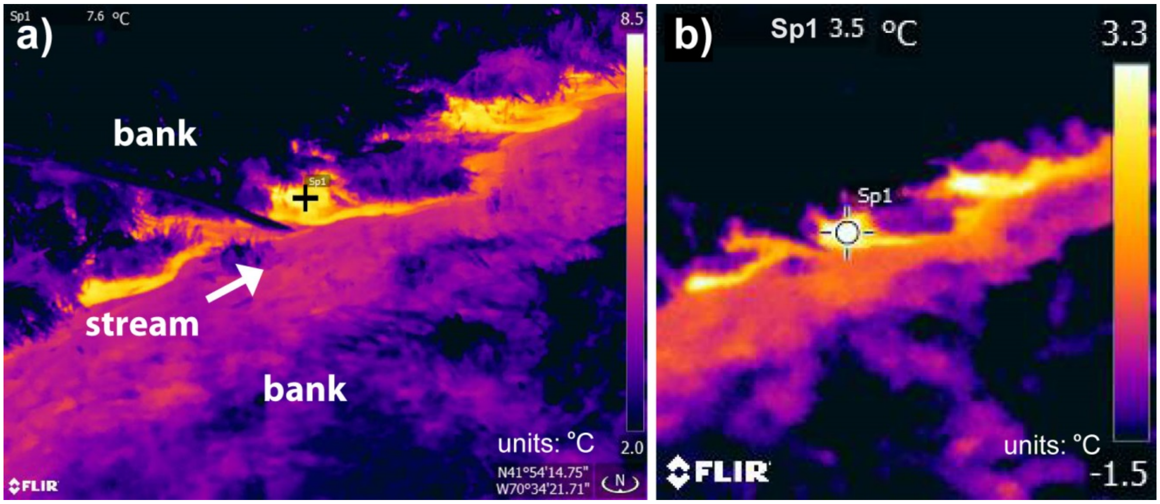

Figure 7. A comparison of TIR images taken in winter at Tidmarsh Farms of GW seepage along the streambank using the a) high-resolution FLIR T640bx, and b) lower resolution FLIR i7 camera models, the cross-hair spots are in approximately the same spatial location between images.

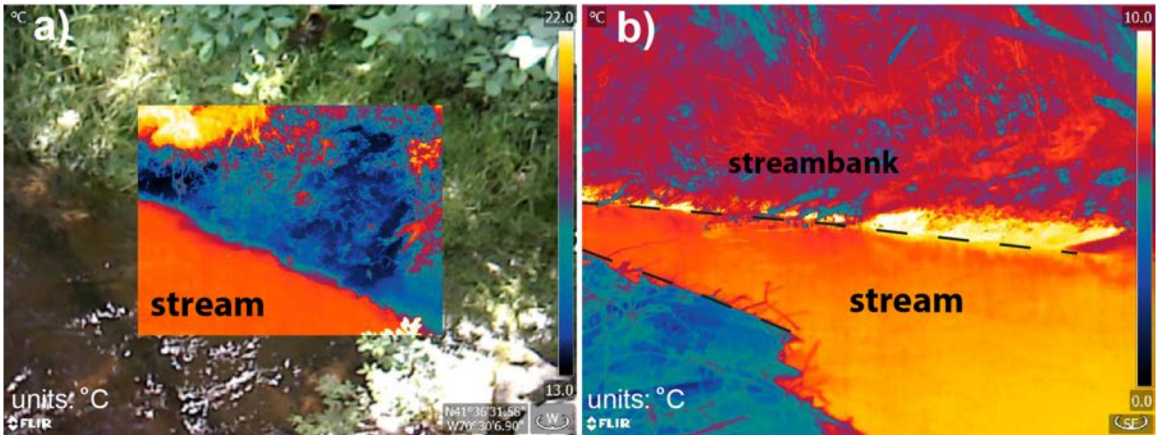

Figure 8. TIR images taken at the Quashnet River at a) in summer at an upstream location showing cold streambank GW seepage with the picture-in-picture view, and b) in winter at a downstream location, showing streambank seepage just above the water line at similar temperature to that observed in panel a). Note, that the stream temperature in a) 20.5°C and in b) the stream temperature is 8.0°C.

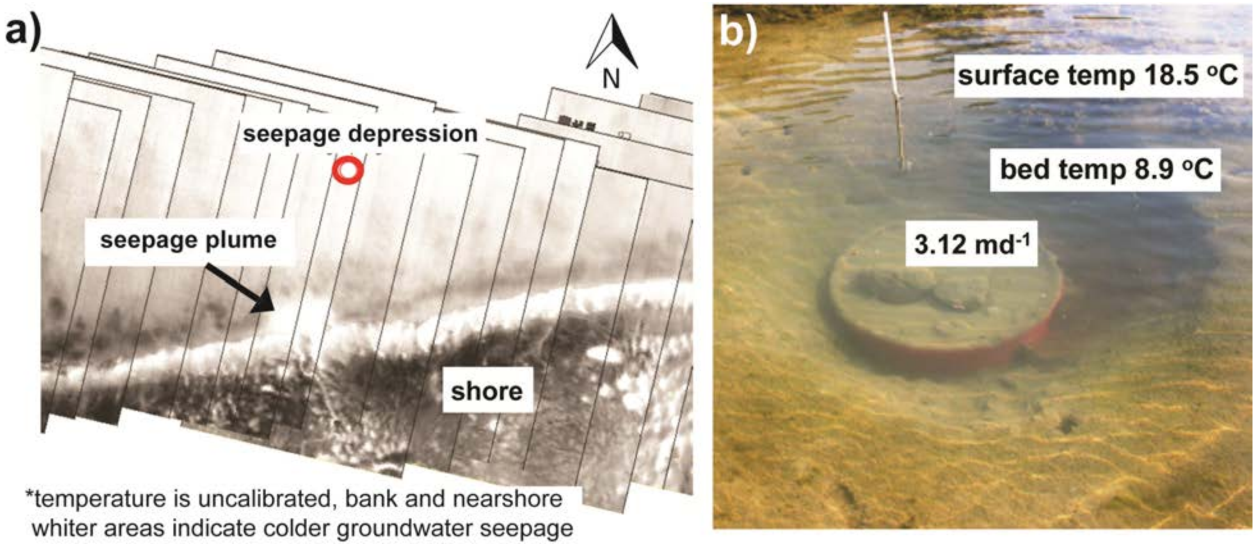

Figure 9: (a) Southern shoreline of Upper Red Rock Lake showing bright white shoreline, darker vegetated land surface to the south, and white lake-surface area to the north.Offshore spring with installed seepage cylinder (b) is shown in (a) with red circle.

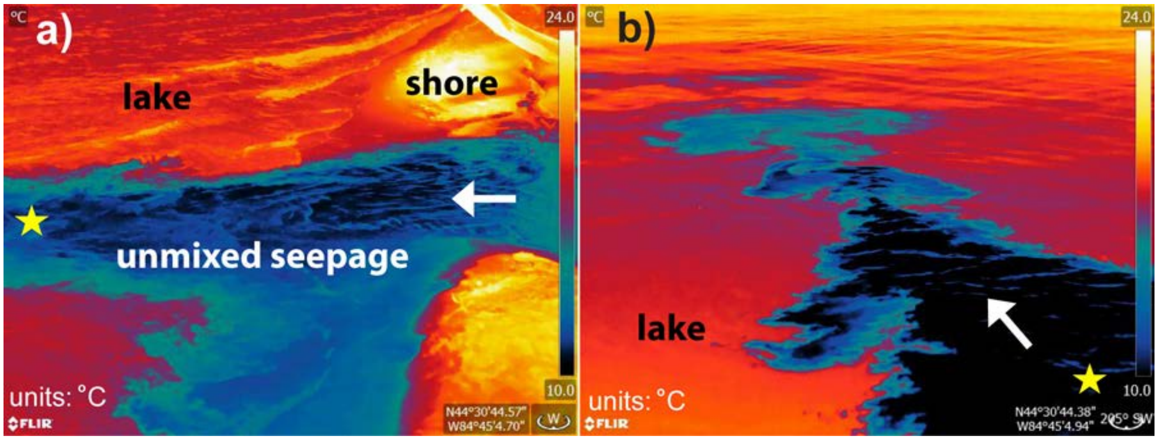

Figure 10. A large tributary of GW seepage to Lake Higgins viewed from a) along the shore and b) away from the shore toward the lake, the star icons are in approximately the same location between images.The cold surfaceGW seepage signature dissipated within 20 m from shore, but was measured directly to occur sub-surface at greater distances than indicated by TIR data alone.

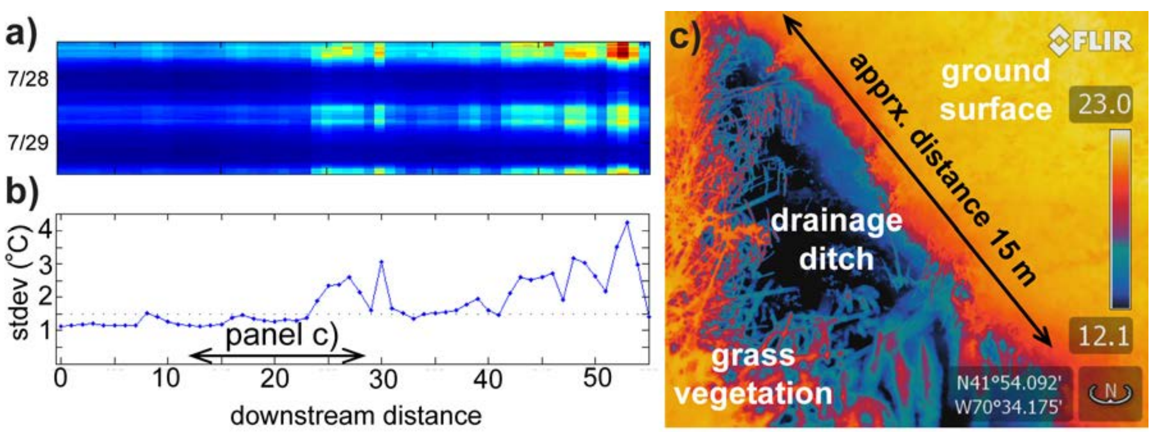

Figure 11.From the zone indicated in Figure 2, a) FO-DTS temperature data over two days collected along a cold drainage ditch with seepage source at 0 m and, b) increasing variance in temperature with distance from the source, c) this snapshot TIR image indicates strong seepage in this drainage ditch but do not capture the temporal subtleties and exact seepage location, the

stream length shown here in TIR approximately corresponds to the stream ditch length shown with the arrow in panel b).

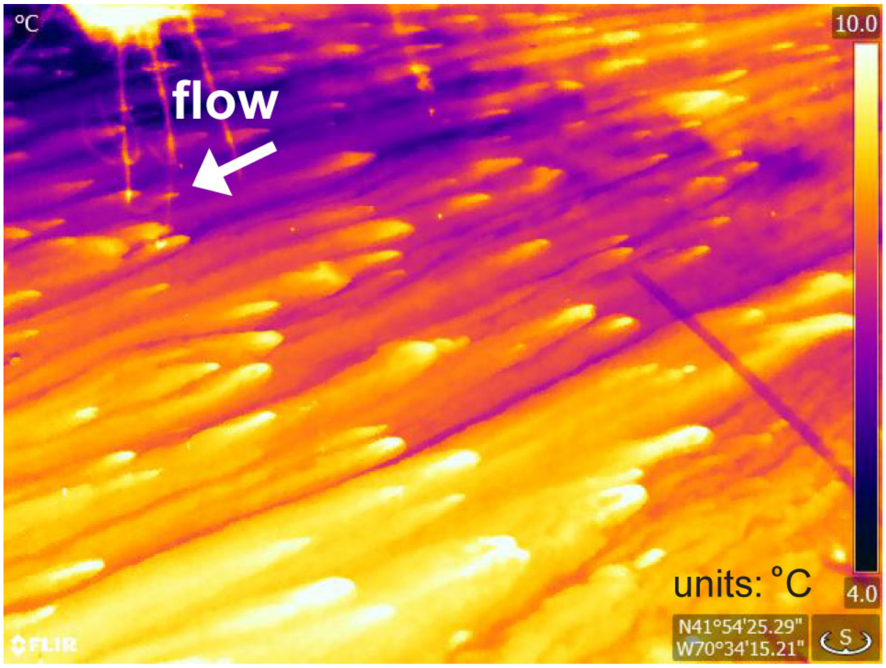

Figure 12.Approximately 1-m wide TIR imagery of shallow (several cm), slowly flowing surface pools on the Tidmarsh peatland surface that shows preferential GW discharge through macropores indicated by focused hotter colors. A similar fine-scale seepage process is captured in Video 1.

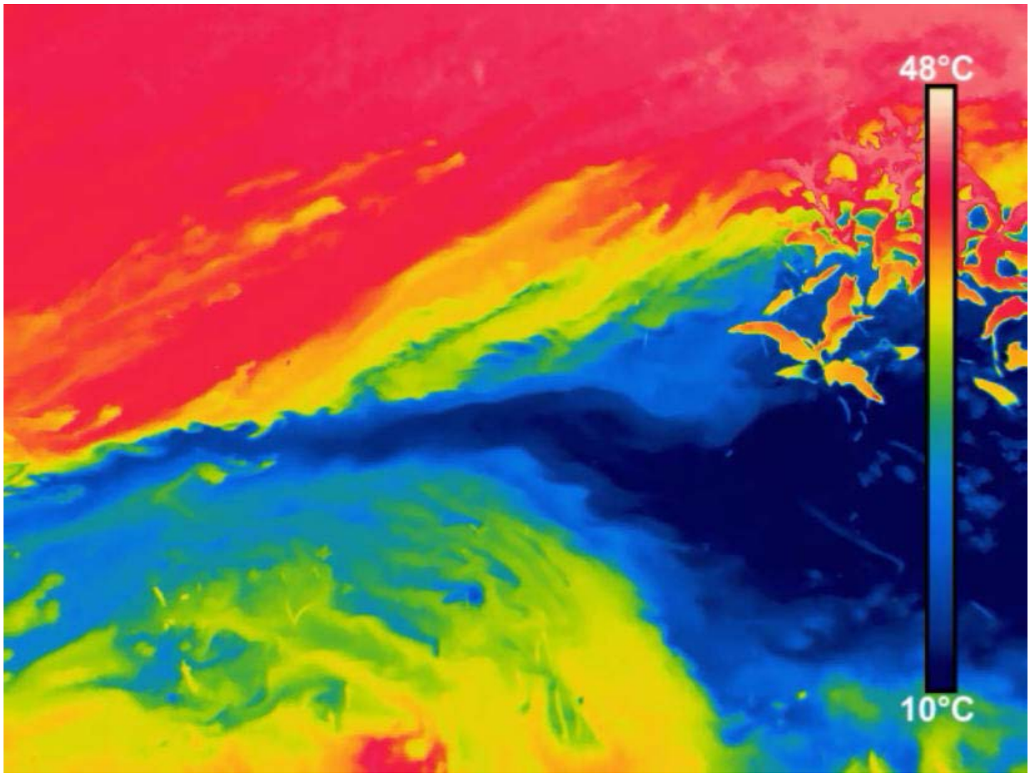

Video 1: TIR video of plunging lower temperature discrete groundwater seepage recorded during the summer at Tidmarsh Farms. Smaller more diffuse macropore seepage can also be observed in the upper left.To access this video component, simply click on the image visible (online version only).

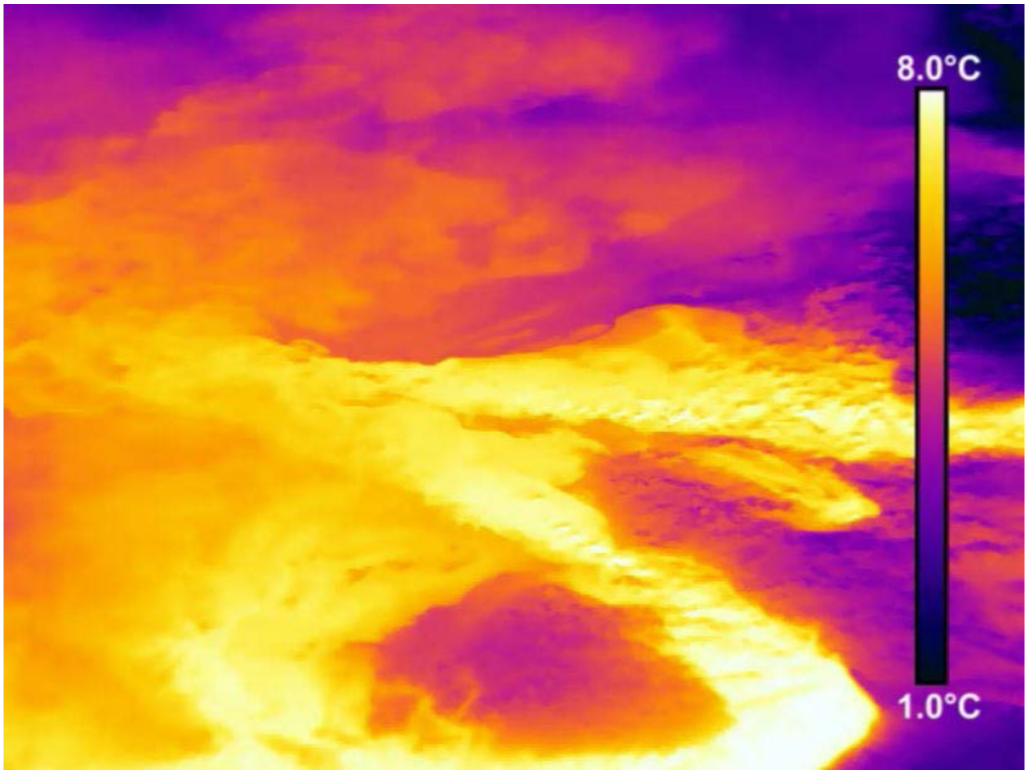

Video 2: TIR video recorded at Tidmarsh Farms during the winter where the warmer groundwater is more buoyant than surrounding surface water. This location is the same discrete groundwater seepage as shown in Video 1. To access this video component, simply click on the image visible (online version only).